X-ray Spectroscopy of Liquid Water Microjets

Kevin R. Wilson,[†] Bruce S. Rude,[‡] Tony Catalano,[‡] Richard D. Schaller,[†] James G. Tobin,[§] Dick T. Co,[†] and R. J. Saykally*,[†]

Department of Chemistry, University of California at Berkeley, Berkeley, California 94720, Lawrence Berkeley National Laboratory, Berkeley, California 94720, and Lawrence Livermore National Laboratory, Livermore, California 94550

Received: December 31, 2000; In Final Form: February 26, 2001

We present the first results from studies of liquid water microjets by soft X-ray absorption spectroscopy. Near the oxygen K-edge (∼530 eV) a fine-structure pattern very similar to that found for gaseous water monomers is observed when the surface-selective total ion yield (TIY) is measured, but a broadened and blue-shifted spectrum emerges when detecting the bulk-sensitive total electron yield (TEY). TIY EXAFS measurements produce a nearest neighbor O−O distance for surface molecules (3.00 Å) slightly longer than that of the isolated water dimer (2.98 Å), whereas the O−O distance extracted from TEY EXAFS corresponds to that accepted for bulk water (2.85 Å). Together, these results evidence an equilibrium liquid water surface dominated by water molecules interacting weakly at longer distances than in the bulk, thus supporting predictions from computer simulations.

Introduction

When a liquid forms an interface, the surface perturbation decays into the bulk with spatial variations on the molecular scale. Of particular interest is the molecular nature of the water liquid/vapor interface, wherein the molecular density changes by many orders of magnitude over several molecular diameters.[1] Dang et al.[2] report molecular dynamics simulations of liquid water showing that the average dipole moment of molecules in this interfacial region rapidly approaches that of gas-phase monomers. Recently, Badyal et al.[3] determined the dipole moment of bulk liquid water to be 2.95 ± 0.6 D, in good agreement with these computer simulations. Dang et al. further report that the average hydrogen bond coordination number per molecule in this surface region to be 2, significantly reduced from the average bulk value of ∼4. Townsend and Rice[1] reached a more dramatic conclusion from their earlier simulations regarding the evolution of the hydrogen-bonding topology through the interface, proposing a restructuring of the hydrogen bond network from the tetrahedrally coordinated bulk to an interfacial shell dominated principally by dimers.

Only recently has it become possible to examine such molecular details of volatile liquid interfaces through experiment. Faubel et al.,[4] achieving nearly collisionless evaporation, determined that the translational energy distribution of molecules evaporating from a 5 μm diameter water microjet surface could be fit by a Maxwellian with $T = -65$ °C. In contrast, larger diameter liquid water microjets exhibited higher surface temperatures limited by collisions originating within the equilibrium vapor blanket surrounding the jet. For example, the surface temperature of a 20 μm diameter jet like that used in the present study was determined to be 0 ± 10 °C.[4] Faubel et al.[5] also measured the valence binding energies of a H_2O microjet surface with ultraviolet photoelectron spectroscopy, finding essentially bulk properties of the outer electron shells with some evidence for a free OH surface component in their spectra. These results are consistent with measurements by Shen et al.,[6] of the equilibrium vapor/liquid interface by sum frequency generation (SFG) spectroscopy, which determined that >20% of the surface water molecules are oriented with one O−H bond extending out of the surface by ca. 38°. These results are in accord with computer simulations that show the liquid surface to be OH terminated[7] and the interface to be ∼1−1.5 molecular diameters thick, consistent with X-ray reflectivity measurements.[8] The effects of surface capillary waves on these interfacial properties is still controversial and the subject of ongoing research.[9]

Experimental Section

X-ray absorption spectroscopy has proven to be a powerful tool for probing the electronic structure of interfaces, but until now it has been prohibitive to apply this approach to volatile liquids. By employing liquid microjet technology, we have been able to transcend these problems and study the water liquid/vapor interface under high vacuum conditions, with near edge X-ray absorption fine structure (NEXAFS) and extended X-ray absorption fine structure (EXAFS) spectroscopic techniques. A schematic of the apparatus used for these liquid microjet studies, conducted at the Advanced Light Source, beamline 9.3.2., Lawrence Berkeley National Laboratory, is shown in Figure 1. The energy range of this beamline spans 20−1000 eV with a photon flux of 10^{11} photons/s/0.1% BW at 400 eV. The chamber consists of three parts (A, B, and C). A differential pumping section A (∼10^{-8} Torr) located upstream of the liquid jet consists of three stages (the final stage omitted for brevity) each pumped by a 70 L/s turbo pump isolated by a series of ∼4 mm conductance limiters. The experimental section B, consists of a 20 μm diameter liquid microjet of H_2O (18 MΩ purity), pressurized to ∼400 psi with an HPLC pump, intersected at 90° with the soft X-ray beam (resolution 0.1 eV.) The TIY and TEY signals were normalized to the incoming photon intensity

* To whom correspondence should be addressed. E-mail: saykally@uclink4.berkeley.edu.
[†] University of California at Berkeley.
[‡] Lawrence Berkeley National Laboratory.
[§] Lawrence Livermore National Laboratory.

10.1021/jp010132u CCC: $20.00
Published on Web 03/31/2001

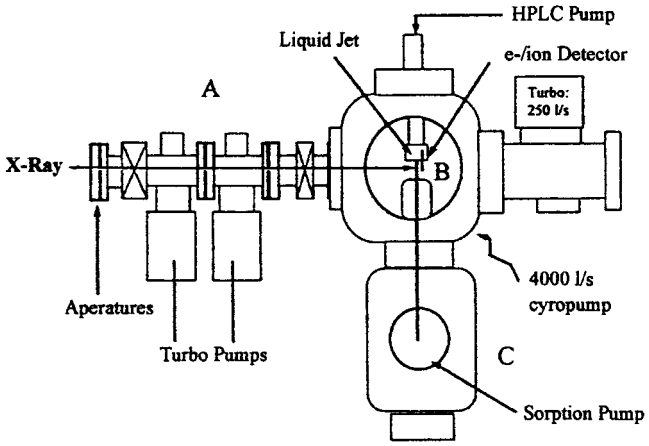

Figure 1. Schematic of the apparatus used for liquid microjet studies conducted at the Advanced Light Source, beamline 9.3.2., Lawrence Berkeley National Laboratory.

(I_o) from a gold grid located upstream of the liquid jet endstation. A ~4000 L/s (water vapor) helium cryopump and a 250 L/s turbo pump maintained the main chamber at $\sim 10^{-4}$ Torr during the liquid jet operation. TIY and TEY detectors are located 1 mm above and below the liquid jet and consist of a detector positioned behind a 0.5 mm aperture that can be independently biased (±0−500 VDC), which serves to spatially filter any contribution from residual water vapor. The TIY and TEY signals are processed by a picoammeter, voltage to frequency converter, and a computer. Absolute energy calibration was obtained from an internal spectral feature in the I_o grid and referenced to a water vapor spectrum obtained in a gas cell located in the final section of the beamline. Absolute energies were determined within 0.5 eV. Region C (10 mTorr) is separated from the interaction region by a 300 μm aperture and is pumped by a ~1000 L/s sorption pump. Spectra of a H_2O liquid microjet measured near the oxygen K-edge are shown in Figure 2 for both TIY and TEY, compared with the TIY for a sample of gas-phase water. The striking similarity between the gas-phase and liquid microjet TIY NEXAFS is immediately apparent.

Results and Discussion

The TIY signal is primarily sensitive to the outermost surface layer, whereas TEY detection probes ~25 Å into the bulk.[10] The sharp fine structure (features A, B, C, D, and E in Figure 2) observed in gaseous H_2O has been assigned[11,12] to a series of dipole transitions of the oxygen 1s core electron to quasi-bound states consisting of pure and mixed valence/Rydberg states just below the ionization potential. The lowest energy NEXAFS states are relatively unperturbed by the molecular environment but can exhibit energy shifts and broadened line widths reflecting intermolecular interactions. The higher states, however, have a large component of spatially extended Rydberg states in their wave functions and are far more sensitive to such perturbations. The liquid microjet TIY NEXAFS spectrum exhibits three peaks (A, B, C) that are unshifted but broadened by 10% relative to their gas-phase analogues, while the other features (D and E) found in the gas-phase spectrum are severely broadened or missing entirely. Such broadening is expected from overlap of these spatially extended Rydberg states with orbitals on nearby molecules. In addition, the K-edge ionization potential of liquid water has been shown to red shift to 538.0 eV from the gas-phase value of 539.7 eV.[5] This final state relaxation effect would place the IP nearly coincident with the observed

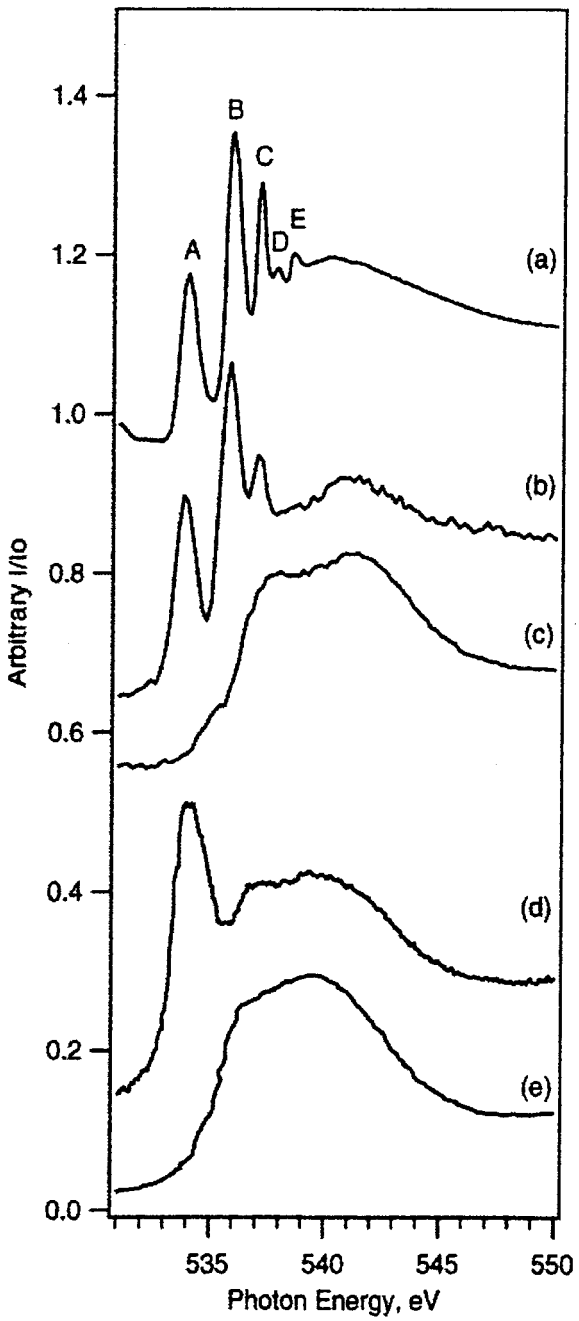

Figure 2. NEXAFS spectra of (a) TIY gas-phase H_2O, (b) TIY, and (c) TEY from a 20 μm liquid microjet. Peaks A and B have been previously assigned in the literature[11,12] to transitions from the $1a_1$ to the mixed $4a_1/3sa_1$ and $2b_2$ states, respectively. C is assigned as a transition to $3pb_1$ and $3pa_1$ symmetry Rydberg orbitals. D is assigned to the $4pb_2$ state with E consisting of transitions to many different orbitals. The peaks labeled A, B, and C in the gas-phase spectrum are clearly present in TIY of the liquid microjet and are significantly broadened and blue shifted in the TEY spectra. Conversely, peaks D and E are absent in the TIY of the microjet. Oxygen K-edge NEXAFS spectra reported by Coulman et al.[13] of ice monolayers measured by (d) H+ and (e) Auger electron yield techniques.

transition energies of peaks D and E and could contribute to lifetime broadening.

For comparison, the low resolution H+ NEXAFS spectrum measured by Coulman et al.[13] for ice monolayers is shown in Figure 2. The sharp peak (A) in the H+ NEXAFS spectrum of ice is also unshifted relative to the gas phase and determined to have an instrumental limited fwhm of 1.5 eV. This feature was assigned by Coulman et al. to surface molecules with reduced

hydrogen bond coordination, consistent with the existence of "dangling" surface OH bonds. The presence of sharp fine structure for both the liquid and ice surface spectra illustrate the high sensitivity of ion yield detection techniques for elucidating surface-localized electronic states. Moreover, peaks B and C are significantly broadened at the ice surface, suggesting significant differences between the structure and perhaps the thickness of the ice and liquid water interface.

The TEY NEXAFS spectrum of the liquid microjet is shifted to higher energy by ~1.0 eV and is severely broadened relative to the gas phase, nearly identical in appearance to spectra previously observed in Auger NEXAFS studies of amorphous ice monolayers shown in Figure 2.[13,14] This broad unstructured spectrum observed in the TEY NEXAFS is consistent with both electronic perturbation resulting from stronger intermolecular hydrogen bonds and greater spatial confinement of the valence/Rydberg wave functions by neighboring molecules, characteristic of hydrogen-bonded condensed phases.

Weak EXAFS oscillations are observed in both the TIY and the TEY measurements (Figure 3). Fourier analysis of the oscillations yield an average nearest neighbor O−O distance of 3.00 ± 0.05 and 2.85 ± 0.05 Å for the TIY and TEY, respectively. The experimental TEY oscillations are in good agreement with previous X-ray transmission studies of bulk water.[15] The TIY measurements, however, evidence a significant lengthening of the O−O distance and consequently an increase in the average hydrogen bond length at the interface. In fact, the O−O distance extracted for the interfacial region is actually slightly larger than that determined for the water dimer by Terahertz VRT spectroscopy.[16] Some tentative evidence for a similar lengthening of the O−O separation is reported for amorphous ice surfaces.[13] In any case, these EXAFS oscillations confirm the condensed-phase origin of the TIY signal and are consistent with the observations of sharp TIY NEXAFS spectra.

The relationship between the surface of liquid microjets and the equilibrium liquid/vapor interface has been discussed in the literature.[4,17,18] It was found that the surface temperature depends sensitively on the number of molecular collisions occurring in the local vapor phase that surrounds the jet. The diameter of this gaseous envelope is calculated to be 5 times the 20 μm jet diameter and is the source of molecular collisions that limit the measured surface temperature to 273 K.[4] Moreover, the equilibrium vapor pressure corresponding to this surface temperature is 4.5 Torr, yielding a mean free path between collisions of ~10 μm. Consequently, molecules in this region will thus make an average of 6 collisions with other gaseous molecules and many collisions with the surface as they traverse this region, after which the vapor density decreases as the reciprocal of the distance from the jet. Under these conditions, the liquid jet surface is very nearly in thermal equilibrium with the local vapor density. Raman and infrared spectra recorded in our laboratory indicate that the average bulk temperature of a 20 μm jet is ~290 K.

The measurements presented here provide the first experimental measure of both the surface relaxation and the dramatic weakening of electronic perturbations due to diminished intermolecular hydrogen bonding at the surface of liquid water. Although, we cannot determine the explicit H-bond geometry at the surface, the 5% lengthening of the average O−O distance to essentially that found for the water dimer is clearly indicative of weaker hydrogen bonds and suggests an interfacial "phase" of relatively more mobile molecules, consistent with computer simulations of the liquid water surface in which the interfacial diffusion constant is predicted to be ~58% greater than the bulk.[1] However, the computed properties of such interfaces are extremely sensitive to the force field used, and clearly require more thorough study in order to quantitatively interpret the new results presented here.

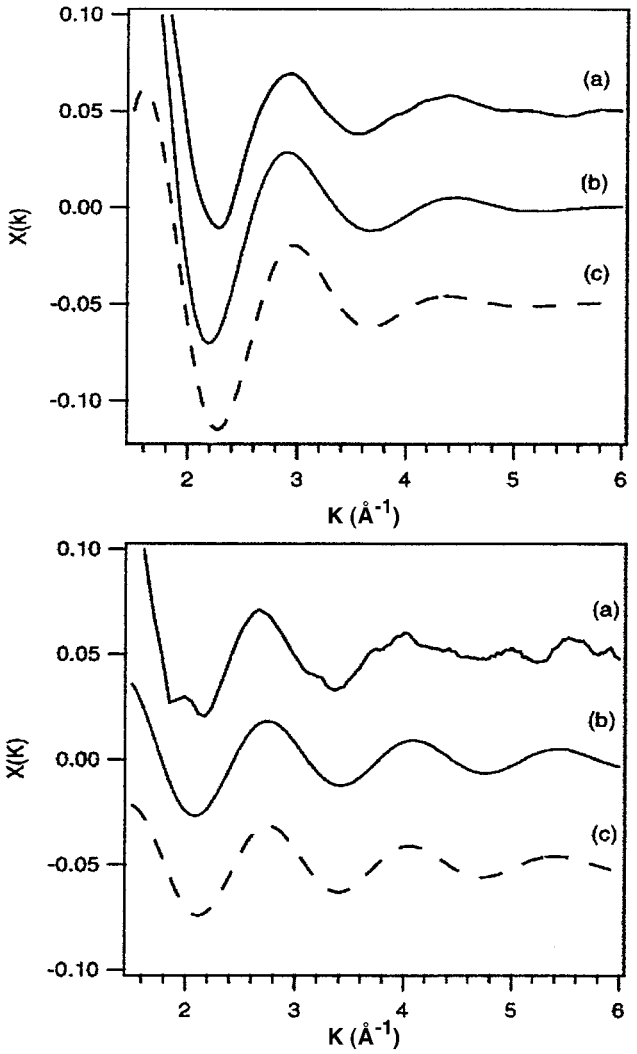

Figure 3. EXAFS spectra measured in a 20 μm diameter liquid jet. (Top panel) TEY EXAFS. (a) Raw data, recorded with an instrumental resolution of $R = 1.0$ eV and smoothed with a five-point Savitzsky-Galoy algorithm. (b) Fourier-filtered oscillation, corresponding to the O−O distance, extracted by standard techniques. (c) Single distance fit to the filtered oscillation using the EXAFS single scattering formalism.[19] The resulting fit yielded a R_{O-O} distance of 2.85 ± 0.05 Å. (Bottom panel) TIY EXAFS. (a) Raw data ($R = 1.0$ eV) smoothed with a five-point Savitzsky-Galoy algorithm. (b) Fourier-filtered oscillation. (c) Single distance fit yielding a R_{O-O} of 3.00 ± 0.05 Å. It should be noted that these EXAFS oscillations were extracted by standard techniques.[20] In addition, both EXAFS fits were parametrized by an O−O phase shift function derived, using the known nearest neighbor distance in liquid water, from Yang and Kirz's bulk water EXAFS study.[15]

Acknowledgment. This work was supported by the Experimental Physical Chemistry Division of the National Science Foundation. We acknowledge the outstanding technical support at the Advanced Light Source, Lawrence Berkeley National Laboratory, Berkeley, CA, specifically Dr. John Bozek, Dr. Eddie Moler, John Pepper, and Steven Klinger. In particular, we are indebted to Tim Williams for his outstanding technical support in the construction of the experimental chamber. We thank Prof. Anders Nilsson for enlightening discussions.

References and Notes

(1) Townsend, R. M.; Rice, S. A. *J. Chem. Phys.* **1991**, *94* (3), 2207.
(2) Dang, L. X.; Chang, Tsun-Mei *J. Chem. Phys.* **1997**, *106* (19), 8149.
(3) Badyal, Y. S.; Saboungi, M. L.; Price, D. L.; Shastri, S. D.; Haeffner, D. R.; Soper, A. K. *J. Chem. Phys*. **2000**, *112* (21), 9206.
(4) Faubel, M.; Schlemmer, S.; Toennies, J. P. *Z. Phys. D.* **1988**, *10*, 269.
(5) Faubel, M.; Steiner, B.; Toennies, J. P. *J. Chem. Phys.* **1997**, *106* (22), 9013.
(6) Du, Q.; Superfine, R.; Freysz, E.; Shen, Y. R. *Phys. Rev. Lett.* **1993**, *70* (15), 2313.
(7) Zakharov, Z.; Brodskaya, E.; Laaksonen, A. *J. Chem. Phys.* **1997**, *197* (24), 10675.
(8) Braslau, A.; Deutsch, M.; Pershan, P. S.; Weiss, A. H. *Phys. Rev. Lett.* **1985**, *54* (2), 114.
(9) Fradin, C.; et al. *Nature* **2000**, *403*, 871.
(10) Bianconli, A. *Appl. Surf. Sci*. **1980**, *6*, 392.
(11) Diercksen, G. H. F.; et al. *J. Chem Phys* **1982**, *76*, 1043.
(12) Kim, D. Y.; Lee, K.; Ma, C. I.; Mahalingam, M.; Hanson, D. M. *J. Chem. Phys*. **1992**, *97* (8), 5915.
(13) Coulman, D.; Puschmann, A.; Hoffer, U.; Steinruck, H. P.; Wurth, W.; Feulner, P.; Menzel, D. *J. Chem. Phys*. **1990**, *93* (1), 58.
(14) Rosenberg, R. A.; et al. *Phys. Rev. B* **1983**, *28* (6), 3026.
(15) Yang, B. X.; Kirz, J. *Phys. Rev. B* **1987**, *36* (2), 1361.
(16) Liu, K.; Cruzan, J. D.; Saykally, R. J. *Science* **1996**, *271*, 887.
(17) Muntz, E. P.; Orme, M. *AIAA J*. **1987**, *25* (5).
(18) Faubel, M.; Kirsters, Th. *Nature* **1989**, 339.
(19) Stern, E. A. *Phys. Rev. B*. **1974**, *10* (8), 3027.
(20) Teo, B. K. *EXAFS: Basic Principles and Data Analysis*; Springer-Verlag: Berlin, 1986.